Engineering 59 (2026) 168–177

Contents lists available at ScienceDirect

Engineering

journal homepage: www.elsevier.com/locate/eng

Research
Low Carbon Transformation for Conventional Energies—Article

# Demonstration of a 5-$MW_{th}$ Chemical Looping Combustion Unit Fueled by Lignite

Zhenshan Li [a,*], Yang Wang [a], Weicheng Li [b], Geng Wei [b], Xinglei Liu [b], Shanhu Lin [b], Jiaye Li [a], Dan Li [a], Qingsong Meng [b], Li Nie [b], Vincent Gouraud [c], Shuting Wei [c], Patrice Font [d], Nils Erland L. Haugen [e], Øyvind Langørgen [e], Yngve Larring [f], Zuoan Li [f], Ningsheng Cai [a]

[a] Key Laboratory for Thermal Science and Power Engineering of the Ministry of Education, Department of Energy and Power Engineering, Tsinghua University, Beijing 100084, China
[b] Dongfang Boiler Co., Ltd., Zigong 643001, China
[c] TotalEnergies, Courbevoie 92400, France
[d] IFP Energies Nouvelles, Lyon 69360, France
[e] SINTEF Energi AS, Trondheim 7491, Norway
[f] SINTEF AS, Oslo 0314, Norway

ARTICLE INFO

*Article history:*
Received 25 December 2024
Revised 27 June 2025
Accepted 10 July 2025
Available online 17 July 2025

*Keywords:*
Carbon capture
Chemical looping combustion
5-$MW_{th}$ demonstration unit
Auto-thermal operation

ABSTRACT

A 5-$MW_{th}$ chemical looping combustion (CLC) unit was designed, built, operated, and demonstrated in China as part of the Chinese–European Emission-Reducing Solutions (CHEERS) project, funded by China's Ministry of Science and Technology (MOST) and the European Union (EU)'s Horizon 2020. In the configuration designed by the Chinese partners, the air reactor (AR) is a transport bed, while the fuel reactor (FR) is a bubbling/turbulent fluidized bed. The solid circulation between the FR and AR is regulated by the overflow method, and the oxygen carrier (OC) from the AR cyclone returns to the FR riser. From June to September 2024, the 5-$MW_{th}$ demonstration unit was operated and tested more or less continuously, with a thermal input ranging from 3.5 to 5.0 $MW_{th}$. During the operation, all solid fuel was fed into the dense bed of the FR, while only air was introduced into the AR. No electric or other external heating was applied, meaning that the whole pilot unit was heated by the oxidation of the OC within the AR. Hence, auto-thermal CLC operation was successfully achieved. Heating the unit was completed in 48 h; furthermore, switching to CLC mode was straightforward and took less than 1 h. During the operation, the temperature of the entire loop was stable. The temperatures of the AR and FR were 1000–1040 °C and 940–980 °C, respectively. Based on the operational data, the maximum $CO_2$ capture efficiency of the lignite-fed CLC unit was greater than 97%, and the minimum oxygen demand for unburnt gases from the FR was 2.45%. This work bridges the gap between lab-scale research and industrial applications in the field of CLC.



## 1. Introduction

The global mean near-surface temperature in 2023 was 1.45 ± 0.12 °C above the pre-industrial average [1], approaching the 1.5 °C target set by the Paris Agreement [2]. Greenhouse gas emissions resulting from human activities are the primary cause of globe warming and climate change. The 2024 Statistical Review of World Energy, released by the Energy Institute, indicates that energy-related greenhouse gas emissions exceeded 40 Gt of $CO_2$ equivalent for the first time in 2023 [3]. $CO_2$ is the main greenhouse gas, primarily originating from the combustion and utilization of fossil fuels. However, the share of fossil fuels in the global energy mix was 80% in 2023 [4], indicating that they still maintain a dominant position. To address global warming and climate change, there is an urgent need to transition from conventional fossil fuel-based energy sources to more sustainable alternatives. This transition demands not only diversifying the energy mix but also integrating advanced technologies to minimize the carbon footprint of carbon-based fuels.

Carbon capture, utilization, and storage (CCUS) technology is a crucial component of global efforts to rapidly mitigate greenhouse

* Corresponding author.
*E-mail address:* lizs@tsinghua.edu.cn (Z. Li).

https://doi.org/10.1016/j.eng.2025.07.017

gas emissions and achieve global carbon neutrality [5]. Carbon capture is a critical process that carries the highest cost in the CCUS chain; its routes include pre-combustion technology, post-combustion technology, oxy-fuel combustion, and chemical looping combustion (CLC). Because of inherent technological limitations, pre-combustion, post-combustion, and oxy-fuel combustion technologies result in power plant efficiency reductions of 6%–11%, 9%–14%, and 7%–11%, respectively [6]. In comparison, CLC is regarded as a promising technology for $CO_2$ capture, with very low energy penalties [7]. For example, Lyngfelt and Leckner [8] predicted the efficiency penalty of a 1000-$MW_{th}$ CLC boiler to be only 3.9%. A CLC unit is primarily composed of an air reactor (AR) and a fuel reactor (FR), while an appropriate solid metal oxide, acting as the oxygen carrier (OC), is circulated between the two reactors to transfer lattice oxygen to fossil and non-fossil fuels [9]. Direct contact between air and fuel is avoided, and the exhaust gas stream from the FR mainly contains $CO_2$ and $H_2O$, such that high-purity $CO_2$ is obtained after $H_2O$ condensation.

About 40 years of research history have passed since a CLC configuration was first proposed by Richter and Knoche in 1983 to improve the combustion efficiency of power plants [10,11]. Megawatt-scale demonstration is a very significant step for CLC industrial application; however, only a very limited number of megawatt-scale CLC pilots exist today. Alstom built a 3-$MW_{th}$ CLC unit in Connecticut, United States [12,13], but no data on auto-thermal chemical looping operation have been published from this unit so far, according to our best knowledge. A 1-$MW_{th}$ CLC unit was built by the University of Darmstadt [14], but it was reported that it was difficult for this 1-$MW_{th}$ unit to maintain auto-thermal operation, and its carbon capture efficiency was relatively low [15]. A 3-$MW_{th}$ CLC pilot with natural gas was built in Republic of Korea [16], and a 3-$MW_{th}$ chemical looping gasification unit was built by Ningxia University in China [17]; however, no public reports on auto-thermal demonstration have been made. Thus, there is a lack of successful auto-thermal demonstrations of megawatt-scale CLC pilots, making this step the major challenge in the commercialization of CLC technology.

To solve this challenge, an international cooperation project named Chinese–European Emission-Reducing Solutions (CHEERS), funded by China's Ministry of Science and Technology (MOST) and the European Union (EU)'s Horizon 2020, aims to achieve auto-thermal demonstration and push the technological frontiers beyond the state of the art [18]. The project has a total of nine partners, of which three are from China (Tsinghua University, the coordinator of the Chinese partners, along with Dongfang Boiler Co., Ltd., and Zhejiang University) and six are from Europe (SINTEF Energy Research, the coordinator, along with SINTEF AS, TotalEnergies, IFP Energies Nouvelles, Bellona, and Silesian University of Technology). Within the CHEERS project, there are two configurations [19]: The EU configuration is optimized for petroleum coke (petcoke) for the European partners, and the Chinese (CN) configuration is optimized for lignite for the Chinese partners. The two configurations share most components, with the carbon stripper (CS), dividing fluidized bed (DFB), and L-valves being the most noticeable exceptions in the EU configuration [19]. In the CN configuration, the solid circulation between the FR and AR is controlled by the overflow method, and the OC from the AR cyclone returns to the FR riser [19].

This study reports the results of the auto-thermal operation of the CN configuration in the 5-$MW_{th}$ CLC unit within the CHEERS project. Norwegian ilmenite was used as the OC and Indonesian lignite was used as the fuel in the 5-$MW_{th}$ CLC pilot, which is the largest CLC unit in the world. Important performance factors, including the carbon capture efficiency ($\eta_{CC}$) and the oxygen demand of the unburnt gases ($\Omega_{OD}$), are calculated to evaluate the results of the CLC tests. The effects of operational parameters—namely, the primary air ratio in the AR and the inventory in the FR—on the oxygen demand ($\Omega_{OD}$) are investigated. An evaluation of $NO_x$ and $SO_2$ emissions from the FR is also presented.

## 2. Experimental section

### 2.1. The 5-$MW_{th}$ CLC demonstration unit

A schematic design of the CLC pilot's CN configuration for the China partners is shown in Fig. 1, and the dimensions of the reactors are summarized in Table 1. Both reactors are lined with refractory materials to minimize heat loss to the surrounding environment. With a superficial gas velocity of 9.5–11.5 $m{\cdot}s^{-1}$ and a solids hold-up ranging from 0.005 to 0.015, the AR operates in the transport bed regime [20]. The total air entering into AR is divided into the primary air and the secondary air. The primary air ratio of the AR and the total bed inventory of the entire system are critical operational parameters for controlling the solid circulation rate [21]. The superficial gas velocity in the loop seals is around 0.2–0.5 $m{\cdot}s^{-1}$, which provides efficient solids passage but offers little capability for regulating the solid circulation rate. The OC from the AR cyclone returns to the FR riser and is transported up into the CS above the FR. The OC within the FR riser, as well as the OC being entrained into the top section above the FR, is used to convert the unburnt gases released from the FR. Especially when a material with an oxygen uncoupling effect is used as the OC, such as synthetic perovskite materials [22,23], the gas-phase oxygen released from the OC can be used to effectively convert the unburnt gases inside the riser and top section. For an OC with two-stage oxidation kinetic behavior, the initial fast stage should be fully used, while the slower second stage is unsuitable for full oxidation because of its very slow kinetics. This is, however, not a problem, since the first-stage oxidation kinetics of ilmenite is fast enough to allow the ilmenite to reach the level of oxidation needed for the oxygen transport required by the lignite combustion [24]. In the CN configuration, all the OC from the AR is transported to the FR [25], and there is no recirculation of the OC returning to the AR itself; this differs from the EU configuration [19], as shown in Fig. 1.

The FR is designed as a bubbling/turbulent fluidized bed, with an operational gas velocity between 1.8 and 3.0 $m{\cdot}s^{-1}$; this results in good gas–solid contact and a high solid circulation rate [26]. The overflow port is located approximately 2.6 m above the distributor plate of the FR, while the fuel feeding port is positioned about 1.1 m above the distributor plate. Solid fuel is fed directly into the dense phase of the FR by a screw feeder to achieve good mixing and contact between the volatiles and OC, which is a key factor in the effective conversion of CO, $H_2$, $CH_4$, char, and so forth. The auto-balance principle of solid circulation is ensured in the CN configuration design; that is, the CLC system can achieve continuous solid circulation without complex controls. The solid circulation between the fuel and ARs is controlled by means of the overflow method, and an overflow port is installed in the FR [26]. The bed height in the FR is higher than the overflow port to prevent the port from constraining the solid circulation rate.

Regarding the challenging issue of char slipping into the AR, it is recognized that the char derived from lignite exhibits good reactivity and a fast gasification rate [27], and the residence time in the FR is long enough for lignite char conversion. Furthermore, the lignite is directly introduced into the dense phase of the FR via a screw feeder, thereby enhancing heat transfer to the fuel and facilitating the gasification of lignite char. In addition, the particle size of lignite is ten to several tens of times larger than that of the OC, which effectively suppresses its overflow from the FR to the AR. It should be noted that one of the critical design features in the

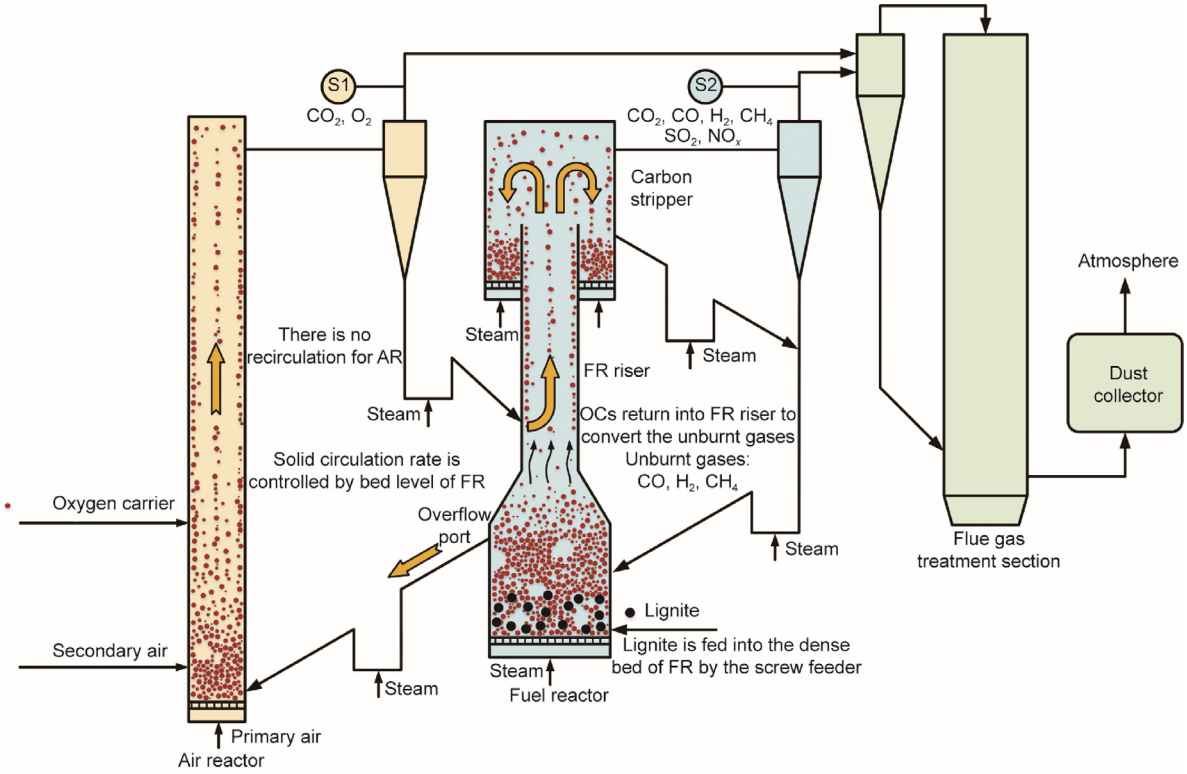


**Fig. 1.** Schematic design of the CLC pilot's CN configuration within the CHEERS project. S1 and S2: gas sampling ports at the outlets of the AR cyclone and FR cyclone, respectively.

**Table 1**
Main dimensions of the 5-$MW_{th}$ pilot.

| Reactor | Height (m) | Inner diameter (m) | Outer diameter (m) |
|---|---|---|---|
| AR | 33.810 | 0.732 | 1.540 |
| FR | 7.740 | 1.490 | 2.040 |
| FR riser | 5.023 | 0.700 | 1.248 |

**Table 2**
Physical properties and composition of the fresh Norwegian ilmenite used in the unit.

| Item | Value |
|---|---|
| Skeletal density ($kg \cdot m^{-3}$) | 4662 |
| Size (μm) | 120–400 |
| $TiO_2$ concentration (wt%) | 42.12 |
| $Fe_2O_3$ concentration (wt%) | 47.37 |
| $SiO_2$ concentration (wt%) | 5.00 |
| $Al_2O_3$ concentration (wt%) | 2.49 |
| MgO concentration (wt%) | 1.87 |

CN configuration is the feeding system of solid fuel, in which solid fuel particles several millimeters in size are fed into the bottom of the FR. This is a major difference from the system used in the EU configuration, in which petcoke powder (with a particle size smaller than 100 μm) is fed into the FR through a pneumatic conveying method [28].

In this unit, no $CO_2$ compression and purification system is applied, and the $CO_2$ in the flue gas from the FR is not captured. The flue gases leaving the cyclones of the AR and the FR are directed into a common downstream cyclone and then enter the flue gas treatment section, where the flue gas is cooled and treated for the removal of nitrogen oxides ($NO_x$) and sulfur oxides ($SO_x$). After passing through the flue gas treatment section, the gas stream enters a dust collector for dust removal before being discharged into the atmosphere, as shown in Fig. 1.

### 2.2. Materials

Ilmenite is a commonly used OC in the CLC field due to its excellent physical stability and stable reactivity. Therefore, Norwegian ilmenite, provided by SINTEF Energi AS, was used as the OC in this experiment. The main physical properties and the composition of the ilmenite are shown in Table 2. Ilmenite undergoes an activation phenomenon in which its reactivity improves after multiple redox cycles [29]. However, it is not easy to activate large quantities of the OC on an industrial scale. Thus, only part of the ilmenite was activated before the experiment. To ensure a successful start-up of the 5-$MW_{th}$ CLC pilot, the activated ilmenite was first injected into the unit. Once the unit entered the auto-thermal CLC mode, fresh ilmenite was used to replenish the loss of OC fines from the unit. Under the operating conditions of the 5-$MW_{th}$ CLC unit, the minimum fluidization velocity of the activated ilmenite is between 0.028 and 0.030 $m \cdot s^{-1}$. The detailed calculation method is provided in Appendix A.

Lignite sourced from Indonesia was selected as the solid fuel for this experiment. The results of the proximate and ultimate analyses of the lignite are summarized in Table 3. This lignite is characterized by high volatile matter and low ash content, and most of the lignite particles are on the millimeter scale. The lignite is fed into the dense bed of the FR, as shown in Fig. 1.

### 2.3. Operational conditions

The 5-$MW_{th}$ CLC demonstration unit underwent the following main processes from the beginning to the CLC mode: heating with natural gas, heating with lignite, switching the fluidizing gas from air to steam, and switching from the air-combustion mode to the CLC mode. During the stage of heating with natural gas, both

**Table 3**
Proximate and ultimate analyses of the Indonesian lignite used in the experiment.

| Analysis | Component | Value | Basis |
|---|---|---|---|
| Proximate | Volatile | 36.84 wt% | As received |
| | Fixed carbon | 26.51 wt% | As received |
| | Moisture | 31.80 wt% | As received |
| | Ash | 4.86 wt% | As received |
| Ultimate | C | 70.32 wt% | Dry ash-free |
| | H | 7.26 wt% | Dry ash-free |
| | O | 21.13 wt% | Dry ash-free |
| | N | 0.93 wt% | Dry ash-free |
| | S | 0.36 wt% | Dry ash-free |
| Other information | Size | 0–5 mm | — |
| | LHV | 15.71 MJ·kg$^{-1}$ | As received |

LHV: lower heating value.

reactors were heated by burning natural gas, and air was used as the fluidizing gas for both reactors and in all loop seals. The activated ilmenite began to be added to the unit. When the temperature of the unit reached 420 °C, the lignite was fed into both reactors, and the supply of natural gas was stopped. The unit entered the stage of heating with lignite. During this stage, the heat released from lignite combustion was used to heat the unit, and solid circulation between the AR and FR was gradually established. When the temperature of the unit reached 950 °C, the unit entered the stage of switching the fluidizing gas from air to steam. The heating of the unit was completed in 48 h. At this point, it was necessary to switch the fluidizing gases in the FR and all loop seals to steam. Then, the unit entered the switching stage from the air-combustion mode to the CLC mode. During the CLC mode, the absence of fuel input to the AR was regarded as a necessary precondition to confirm that the unit was operating under autothermal conditions. Therefore, during the CLC stage, it was necessary to stop the fuel supply to the AR, and all fuel was fed into the FR. In this experiment, the unit was operated in the auto-thermal CLC mode for 20 h.

Depending on the operation conditions, three cases were investigated, as listed in Table 4. In all three cases, only lignite was used as the fuel, with no natural gas or any electric heating for this operation; only the solid circulation between the AR and the FR was used to maintain the temperature of the FR. The thermal input of the unit was 3.5–5.0 MW. Correspondingly, the flow rate of air into the AR was 4500–5000 Nm$^3$·h$^{-1}$. The air was preheated to 150 °C using an air preheater before it entered the reactors and the loop seals; the temperature of the steam was 300 °C.

### 2.4. Evaluation parameters

To evaluate the carbon capture performance of the 5-MW$_{th}$ CLC unit, carbon capture efficiency was employed as a quantitative indicator. There are two different definitions for carbon capture efficiency [9]. The first definition specifies how much of the carbon introduced with the solid fuel is captured in gaseous form at the FR outlet, as shown in Eq. (1):

$$\eta_{CC} = \frac{\dot{m}_{C,FR}}{\dot{m}_{C,in} - \dot{m}_{char,out}} = 1 - \frac{\dot{m}_{C,AR}}{\dot{m}_{C,in} - \dot{m}_{char,out}} \quad (1)$$

**Table 4**
Overview of typical operational cases.

| Case | General information | Duration (h) |
|---|---|---|
| Case 1 | Air-combustion mode with all fuels fed into the AR | 24 |
| Case 2 | Switching from air-combustion mode to CLC mode | 6 |
| Case 3 | Auto-thermal operation of the CLC mode with all fuels fed into the FR | 20 |

where $\dot{m}_{C,in}$ refers to the mass flow of the carbon in the solid fuel fed into the FR, $\dot{m}_{C,AR}$ is the mass flow of the carbon flowing into the AR, $\dot{m}_{C,FR}$ represents the mass flow of carbon converted to gaseous form in the FR, and $\dot{m}_{char,out}$ is the mass flow of carbon that escaped the unit in the form of unconverted char.

The second definition is alternatively referred to as the oxide oxygen fraction ($\eta_{OO}$). This parameter is defined as the amount of oxygen used to oxidize the OC in the AR divided by the sum of the oxygen used to oxidize both the OC and the char reaching the AR from the FR, as shown in Eq. (2).

$$\eta_{OO} = \frac{(0.21 - y_{O_2} - y_{CO_2})_{AR,out}}{(0.21 - y_{O_2} - 0.21 \cdot y_{CO_2})_{AR,out}} \quad (2)$$

where $y_{O_2}$ and $y_{CO_2}$ refer to the $O_2$ and $CO_2$ concentrations measured at the AR outlet, respectively.

The oxygen demand ($\Omega_{OD}$) indicates the fraction of oxygen that is lacking to achieve complete combustion of the combustible gas produced in the FR. It can be calculated as follows:

$$\Omega_{OD} = \frac{(0.5 \cdot y_{CO} + 0.5 \cdot y_{H_2} + 2 \cdot y_{CH_4})_{FR,out}}{\Phi_0 (y_{CO} + y_{CO_2} + y_{CH_4})_{FR,out}} \quad (3)$$

where $y_{CO}$, $y_{H_2}$, and $y_{CH_4}$ are the CO, $H_2$, and $CH_4$ concentrations measured at the FR outlet in the absence of water vapor, respectively. $\Phi_0$ refers to the ratio of moles of oxygen needed to convert the fuel completely per mole of carbon in the fuel.

Solid carbon conversion ($\eta_{SC}$) is defined as the fraction of the carbon in the solid fuel that is converted to gas in the entire system, including the AR and the FR. It can be expressed as follows:

$$\eta_{SC} = \frac{\dot{m}_{C,in} - \dot{m}_{char,out}}{\dot{m}_{C,in}} \quad (4)$$

Char conversion ($\eta_{char}$) describes the fraction of the char that is converted to gas in the entire system; it is defined as

$$\eta_{char} = \frac{\dot{m}_{char,in} - \dot{m}_{char,out}}{\dot{m}_{char,in}} \quad (5)$$

where $\dot{m}_{char,in}$ refers to the mass flow of the fixed carbon in the solid fuel fed into the FR.

Elutriated fines from the 5-MW$_{th}$ demonstration unit were collected using a bag dust collector, and the amount of fines was quantified at regular intervals. The fines consisted of OC, fly ash, and unconverted char. The mass flow of the char elutriated from the CLC system can be calculated by the following equation:

$$\dot{m}_{char,out} = \dot{m}_{fines,out} W_{char} \quad (6)$$

where $\dot{m}_{fines,out}$ refers to the mass flow of the fines elutriated from the CLC unit, and $W_{char}$ represents the char content in the fines, measured using a fixed-bed reactor. A detailed description of the experimental apparatus and procedures is provided in Appendix A.

## 3. Results and discussion

### 3.1. Case 1: Air-combustion mode

In Case 1, the unit was operated in the air-combustion mode, and lignite was fed into the AR only and not into the FR. The oxygen gas ($O_2$) concentration at the AR outlet was measured using a zirconia oxygen concentration analyzer. The temperature, pressure drop, fuel feed rate, and $O_2$ concentration at the AR outlet are shown in Fig. 2, which shows the four stages in Case 1.

In Stage 1, lignite was fed into both the AR and the FR. The fuel feed rate for the FR was gradually reduced from 272 kg·h$^{-1}$ to 0, while that of the AR was gradually increased from 427 to 750 kg·h$^{-1}$ at the same time. During Stage 1, there were some fluctuations in

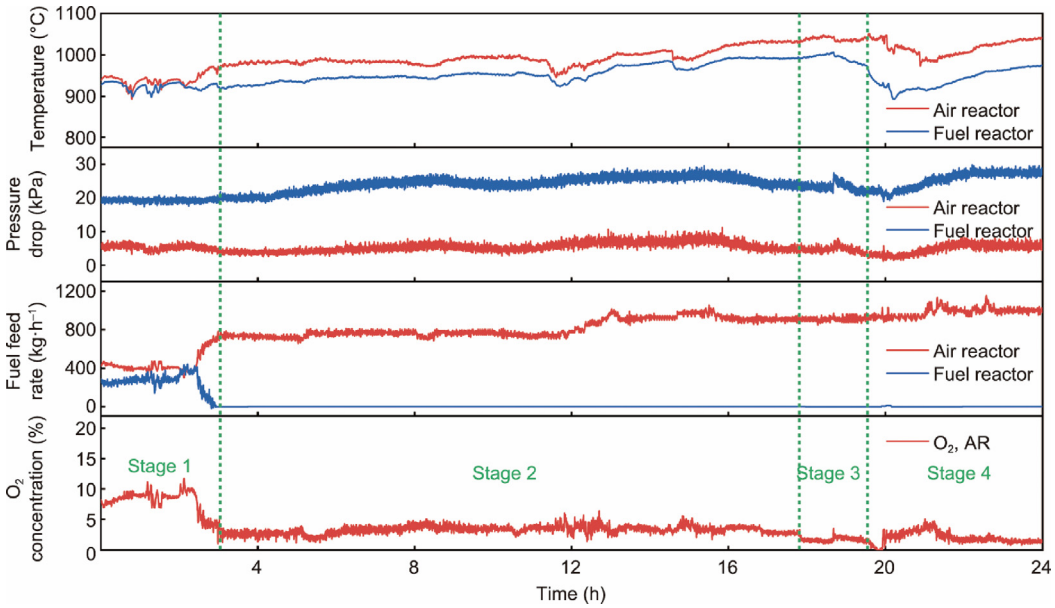


**Fig. 2.** Results for the air-combustion mode (Case 1).

the temperatures of both reactors, but the temperature remained above 900 °C. The $O_2$ concentration at the AR outlet was gradually reduced from 8.17% to 3.94%.

In Stage 2, the fluidizing gas of both reactors was air. The temperature and pressure drop of the reactors were very stable. The temperature in the AR ranged between 950 and 1035 °C, while that in the FR ranged between 920 and 990 °C. The pressure drop in the AR ranged between 3 and 9 kPa, while that in the FR ranged between 20 and 28 kPa. The $O_2$ concentration at the AR outlet was generally maintained between 1.6% and 4.5%.

In Stage 3, the fluidizing gas in the FR and in all the loop seals was gradually switched from air to steam. To ensure stable operation, the switching process was not instantaneous. The temperature and pressure drop in the AR and the oxygen concentration were very stable, but there was a slight decrease in the temperature of the FR when steam was introduced into the FR. This was attributed to the temperature of the steam being lower than the temperature in the FR and to the heat capacity of steam being greater than that of air. The pressure drop in the FR also fluctuated due to the switching of the fluidizing gas.

In Stage 4, the fluidizing gas in the FR and in all the loop seals was steam. The temperature of the FR decreased from 970 to 895 °C, which was related to the temperature and heat capacity of steam. Moreover, the AR temperature decreased slightly, and the temperature difference between the two reactors increased. The solid circulation rate is a powerful tool for regulating the temperature difference between the two reactors. Therefore, to increase the solid circulation rate, ilmenite was added to the unit, causing the pressure in the two reactors to drop further. Consequently, the temperature of the FR gradually increased. To increase the temperature of the whole unit, the fuel feed rate for the AR was increased from 890 to 1024 $kg·h^{-1}$. As a result, the temperatures of the AR and FR increased to 1024 and 975 °C, respectively.

In Case 1, lignite was only fed into the AR, and the heat released in the AR was used to maintain the temperature of the whole pilot unit. The FR temperature was maintained by the OC's sensible heat transferred from the AR. The heat balance in this case was very similar to that in the auto-thermal CLC mode. During Case 1, the temperatures of the two reactors were successfully maintained and even rose to above 950 °C after the fluidizing gas was switched. The operation of Case 1 provided key experience for the subsequent auto-thermal operation of the CLC mode.

### 3.2. Case 2: Switching from air-combustion to auto-thermal CLC mode

During Case 2, the operation condition was switched from the air-combustion mode to the CLC mode—a switch that was critical for the CLC demonstration. Fig. 3 presents the results of Case 2, including the temperature and pressure drop, fuel feed rate, and $O_2$ concentration at the AR outlet. During Case 2, only the fluidizing gas for the AR was air; the fluidizing gas in the FR and in all the loop seals was steam. Fig. 3 illustrates the three stages in Case 2.

In Stage 1, the unit was operated in the air-combustion mode. The temperature of the AR gradually increased from 1000 to 1040 °C, while that of the FR increased from 940 to 975 °C. The pressure drops in the AR and the FR were very stable, at 4.4–7.2 kPa in the AR and 26.2–28.7 kPa in the FR. The lignite was only fed into the AR, and the $O_2$ concentration at the AR outlet was less than 2.5%.

In Stage 2, the fuel feed rate for the FR was gradually increased; at the same time, the fuel feed rate for the AR was gradually decreased, until all fuel was fed into the FR. The heat released in the AR gradually shifted from lignite combustion to OC oxidation. The AR temperature decreased from 1042 to 1003 °C, and the FR temperature decreased from 975 to 958 °C. Notably, both reactors still maintained high temperatures, ensuring the occurrence of the redox reaction of the OC, as well as the pyrolysis and gasification reactions of the solid fuel. The $O_2$ concentration at the AR outlet increased from 2.6% to 6.4%. It can be seen from Fig. 3 that the time for the switching process was about 45 min, and this switch time can be further shortened. The results from Figs. 2 and 3 indicate that the actual operation during the switching process from normal air combustion to the CLC mode is relatively easy in the CN configuration.

In Stage 3, all lignite was fed to the FR; in other words, the unit was operated in the CLC mode. At first, because lignite was no longer being fed to the AR, the oxygen concentration at the AR outlet increased significantly, reaching a maximum value of 12.7%. Moreover, the temperature of the AR decreased to 974 °C. Then, due to the oxidation of the OC, the $O_2$ concentration at the AR

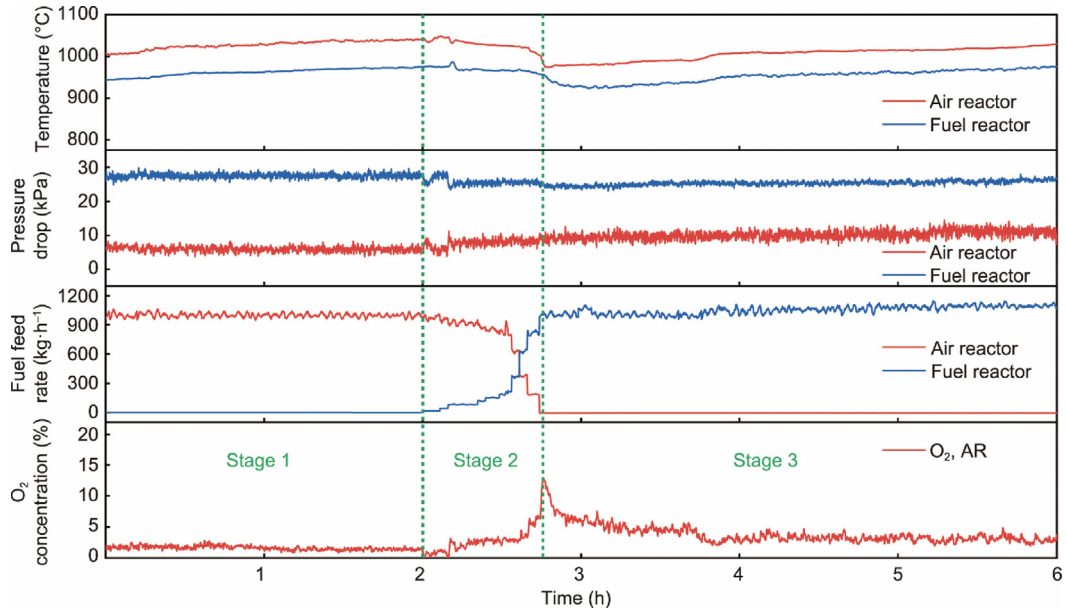


**Fig. 3.** Results for the switching process from the air-combustion mode to the auto-thermal CLC mode (Case 2).

outlet gradually decreased, and the AR temperature gradually increased. The temperature of the FR first decreased and then increased. Pyrolysis and gasification of the lignite occurred, releasing reductive gases in the FR that reduced the OC. These reactions are all endothermic reactions; therefore, the temperature of the FR decreased. Meanwhile, the sensible heat of the OC from the AR maintained the FR temperature. After multiple redox reaction cycles, the reactivity of the OC was further improved, leading to a gradual increase in the temperature of the FR. The temperature of the reactors was maintained above 925 °C for 3.25 h, which indicated that auto-thermal operation of the unit was achieved.

In this case, the operation condition of the unit was successfully switched from the air-combustion mode to the auto-thermal CLC mode. The reactions occurring in the AR smoothly transitioned from lignite combustion to OC oxidation. Moreover, the feeding of lignite into the FR did not cause a dramatic drop in the temperature of the FR.

### 3.3. Case 3: Operational results for the auto-thermal CLC mode

During Case 3, the unit was operated in the auto-thermal CLC mode for 20 h. Lignite was only fed to the FR, and no fuel was fed to the AR. The fluidizing gas in the FR was steam, and no air was introduced into the FR. The heat for the FR was supplied by the circulated OC from the AR. When determining the gas concentration at the outlet of the FR, the sampled gas was extracted, cooled, and dried before being introduced into the analyzer; therefore, the gas concentration was measured in the absence of steam. It should be noted that the gas concentration results were obtained without the application of oxy-polishing. Fig. 4 presents the results for Case 3, including the temperature and pressure drop of the reactors, the gas concentrations at the AR outlet and the FR outlet, the carbon capture efficiency, and the oxygen demand of the unburnt gases. To evaluate the performance of the unit, it was necessary to monitor the gas concentrations at the AR outlet and the FR outlet continuously. However, during the maintenance of the gas analyzers, the gas concentration data was not recorded. The data before and after the maintenance of the gas analyzers are thus connected using dashed lines in Fig. 4.

During the auto-thermal CLC mode, the unit operated very steadily. The thermal input remained stable at approximately 5 $MW_{th}$. The AR temperature was mainly in the range of 1000–1040 °C, and the FR temperature was mainly in the range of 940–980 °C. Because the FR was heated by the OC's sensible heat transported from the AR, the FR temperature showed a highly consistent correlation with the AR temperature. The temperature difference between AR and FR was mainly in the range of 50–70 °C. The pressure drop of the AR mainly varied between 6 and 16 kPa, while the pressure drop of the FR mainly varied between 23 and 28 kPa. The pressure drop reflects the bed inventory and the solid circulation of the unit. Due to the larger size of the FR, the bed inventory in the FR contributed a larger proportion of the total bed inventory in the unit. The OC overflowed from the FR to the AR, and the pressure drop variation in the AR was greatly influenced by that in the FR. The $O_2$ concentration at the AR outlet was mainly in the range of 2%–8%, while the $CO_2$ concentration at the AR outlet was mainly below 2%. The $O_2$ concentration depended on the oxidation of the OC and the combustion of the char that overflowed from the FR, while the $CO_2$ concentration only depended on the char combustion. Because of the significant difference in the particle sizes of the lignite and the OC, the lignite fed to the FR was predominantly distributed at the bottom and underwent pyrolysis and gasification. Moreover, the lignite had a high volatile content and its char exhibited high gasification reactivity, resulting in a relatively low char concentration in the FR. Therefore, only a small amount of char was carried by the OC into the AR. The $CO_2$ concentration at the FR outlet was mainly in the range of 88%–96%. The concentrations of CO and $H_2$ were very similar and varied between 2% and 5%. The $CH_4$ concentration was relatively low, mainly below 2%. The gas concentrations at the FR outlet were associated with the conversion of combustible gas by the OC. The lignite was directly introduced into the middle and lower regions of the dense phase in the FR, facilitating sufficient interaction between the released combustible gases and the OC and thereby increasing the conversion of the combustible gases. The carbon capture efficiency primarily ranged between 91% and 98%, slightly higher than the oxide oxygen fraction, which was mainly within the range of 90%–97%. This discrepancy was mainly attributed to the hydrogen

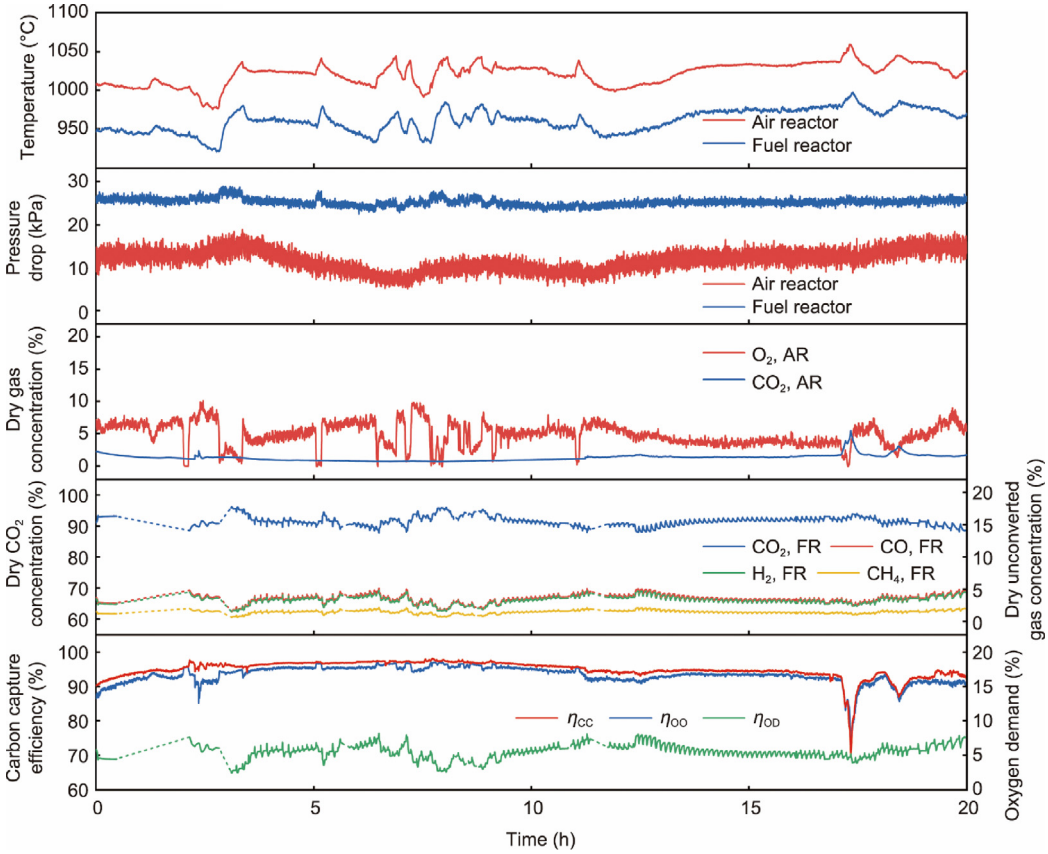


**Fig. 4.** Results for the auto-thermal CLC mode (Case 3).

content in the fuel and the extent of combustible gas conversion in the FR. The oxygen demand of the unburnt gases was mainly in the range of 3%–8%. To the best of our knowledge, this is the first instance worldwide in which the long-term auto-thermal operation of CLC with high carbon capture efficiency and low oxygen demand has been achieved.

Temperature is one of the most critical parameters in the operation of the CLC unit, as it has a significant impact on the reaction kinetics in the unit. Between 8.85 and 11.92 h, the temperature exhibited an overall downward trend. The AR temperature decreased from 1043 to 998 °C, and the FR temperature decreased from 981 to 939 °C. The $CO_2$ concentration at the AR outlet slightly increased from 0.82% to 1.36%. The $CO_2$ concentration at the FR outlet showed an obvious decrease, from 95.29% to 88.99%, while the unburnt gas concentration at the FR outlet showed an obvious increase (CO: 2.01%–4.65%, $H_2$: 1.84%–4.40%, $CH_4$: 0.85%–1.96%). Consequently, the carbon capture efficiency decreased from 97.00% to 94.53%, the oxide oxygen fraction decreased from 96.39% to 91.88%, and the oxygen demand increased from 3.02% to 7.24%. Between 11.92 and 17.08 h, there was an overall upward trend in the temperature. The AR temperature increased from 998 to 1037 °C, while the FR temperature increased from 939 to 979 °C. The $O_2$ concentration at the AR outlet decreased from 7.23% to 3.57%. The $CO_2$ concentration at the FR outlet showed an obvious increase, from 88.09% to 92.93%, while the unburnt gas concentration at the FR outlet showed an obvious decrease (CO: 5.06%–2.88%, $H_2$: 4.70%–2.73%, $CH_4$: 2.13%–1.21%). As a result, the carbon capture efficiency increased from 93.70% to 94.89%, the oxide oxygen fraction increased from 91.05% to 93.85%, and the oxygen demand decreased from 8.03% to 4.55%. The decrease in temperature slowed the reactions between the combustible gases and the OC, resulting in a decrease in the $CO_2$ concentration and an increase in the unburnt gas concentration at the FR outlet. The more complete the conversion of combustible gases in the FR was, the lower the oxidation state of the OC entering the AR would be. Consequently, more oxygen was consumed in the AR, resulting in a lower oxygen concentration at the AR outlet. Therefore, the increase in temperature led to a decrease in the $O_2$ concentration at the AR outlet.

The pressure drop in the AR reflects the solid circulation between the two reactors. Between 3.40 and 6.41 h, the pressure drop in the AR decreased from 14.97 to 7.73 kPa. Because the heat required to maintain the FR temperature was solely provided by the sensible heat carried by the OC, the decrease in solid circulation led to a reduction in the heat entering the FR, which was reflected in the decrease in the FR temperature (from 978 to 933 °C) and the increase in the temperature difference between the two reactors (from 56 to 71 °C). Consequently, the $CO_2$ concentration at the FR outlet decreased from 95.23% to 88.54%, and the concentrations of unburnt gas increased (CO: 1.94%–4.84%, $H_2$: 1.85%–4.40%, $CH_4$: 0.83%–2.04%). The oxygen demand increased from 2.93% to 7.51%. Because of the decrease in FR temperature, the conversion of the combustible gas deteriorated and the degree of reduction of the OC decreased. Moreover, the bed inventory in the AR decreased. Ultimately, the $O_2$ concentration at the AR outlet increased from 3.40% to 7.10%.

It is worth noting that the current pilot unit has certain limitations in its control system, such as an extensive use of manual valves and the use of a single blower for both primary and secondary air in the AR. These limitations may lead to limited control accuracy and slower system response, which can further cause fluctuations during operation, as shown in Fig. 4. However, it should be emphasized that these are not inherent limitations or unavoidable features of CLC technology. In future commercial-scale CLC plants, most of these control issues can be effectively addressed.

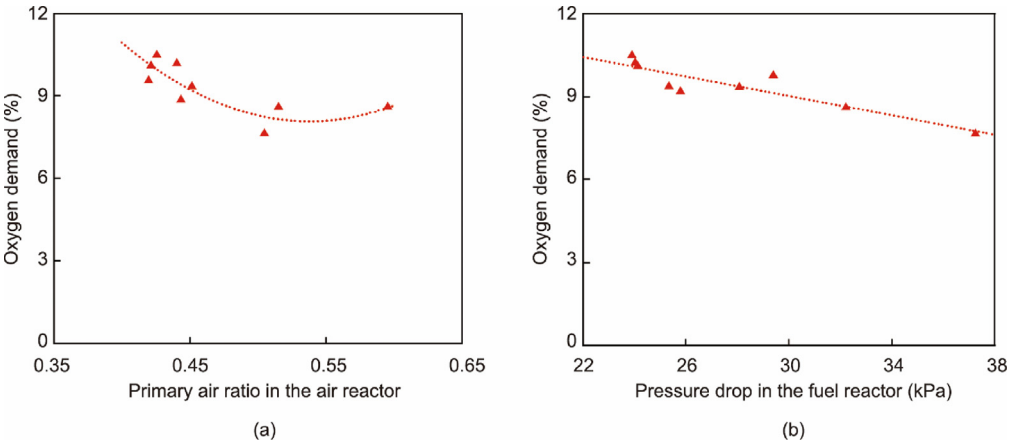


**Fig. 5.** Influence of the (a) primary air ratio in the air reactor and (b) bed inventory of the fuel reactor.

### 3.4. Influence of the primary air ratio in the air reactor and inventory of the fuel reactor

The oxygen demand of the unburnt gases was dependent on the primary air ratio in the AR and the pressure drop in the FR (which can reflect the FR inventory), as shown in Fig. 5. Fig. 5(a) shows that the primary air ratio in the AR had a noticeable influence on the unit's performance. When the primary air ratio was below 0.51, the oxygen demand of the unburnt gas decreased as the primary air ratio increased. In contrast, when the primary air ratio in the AR was greater than 0.51, the oxygen demand appeared to increase as the primary air ratio increased. However, due to the limited number of data points, this trend is not very pronounced. This limitation resulted from the design of the air-supply system, in which both the primary and secondary air were supplied by a single blower. Because the primary and secondary air operated under different pressure conditions, it was difficult to adjust the primary air ratio in the AR, resulting in a limited number of experimental data points. Nevertheless, the current results indicate that the primary air ratio in the AR has a certain impact on the unit's performance. Varying the primary air ratio affects the distribution and residence time of the OC in the AR, thereby affecting its oxidation reaction. This subsequently changes the oxidation state of the OC entering the FR and ultimately affects the conversion of combustible gases. Therefore, investigating the effect of the primary air ratio is meaningful for optimizing unit performance. In future work, the 5-$MW_{th}$ CLC unit will be modified to enable a more detailed investigation of the effects of the primary air ratio in the AR, with the aim of elucidating its influence mechanism and operational characteristics.

In addition, as shown in Fig. 5(b), the oxygen demand of the unburnt gases decreased as the pressure drop in the FR increased. This was because an increase in the pressure drop indicated an increase in the bed inventory, which extended the reaction time between the OC and the combustible gases. Therefore, a larger bed inventory in the FR is conducive to the conversion of combustible gases.

### 3.5. Conversion of solid carbon and char

During the auto-thermal CLC mode, the elutriated fines from the unit were collected in a bag dust collector, with samples taken every 3 h for analysis. The char content in the samples was measured using a fixed bed (a detailed experimental procedure and typical results are provided in Appendix A). During the auto-thermal CLC mode, six samples were collected and numbered in chronological order. As shown in Fig. 6, the char content in the samples was very low, not exceeding 0.39 wt%. In Sample 6, the char content was only 0.11 wt%. Using the char content results, the solid carbon conversion and the char conversion can be calculated according to Eqs. (4) and (5).

The solid carbon conversion and the char conversion of the 5-$MW_{th}$ unit are shown in Fig. 7; the former ranged within 99.69%–99.94%, while the latter ranged within 99.48%–99.90%. The conversion of the solid fuel and char fed into the FR was highly complete, which was closely related to the significant difference in the particle sizes of the lignite and the OC. The lignite fed to the FR was predominantly distributed at the bottom, making it difficult for it to reach the overflow port. The bed materials in the FR were in a bubbling/turbulent fluidized-bed state, with good heat and mass transfer characteristics. The solid fuel and the char were highly pyrolyzed and gasified to generate the combustible gas in the FR.

### 3.6. $NO_x$ and $SO_2$ emissions

It is necessary to focus on the emissions from both the AR and FR. Since the carbon capture efficiency was high, and only a very small amount of char was transferred from the FR to the AR, it can be reasonably assumed that the $NO_x$ and $SO_2$ emissions could be significantly reduced with a high carbon capture efficiency (> 90%), which would also lead to lower $SO_2$ and $NO_x$ emissions

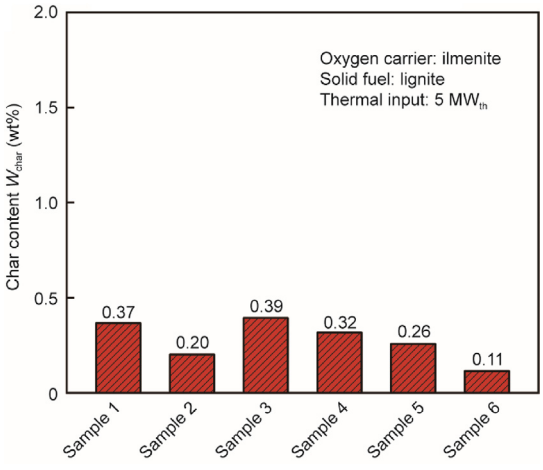


**Fig. 6.** Char content in the fines collected in the bag dust collector.

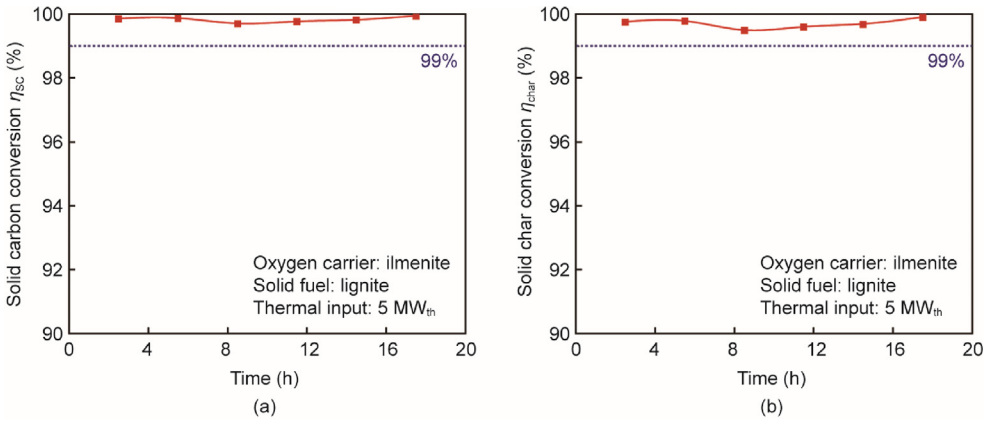


**Fig. 7.** (a) The solid carbon conversion and (b) char conversion of the 5-$MW_{th}$ CLC unit.

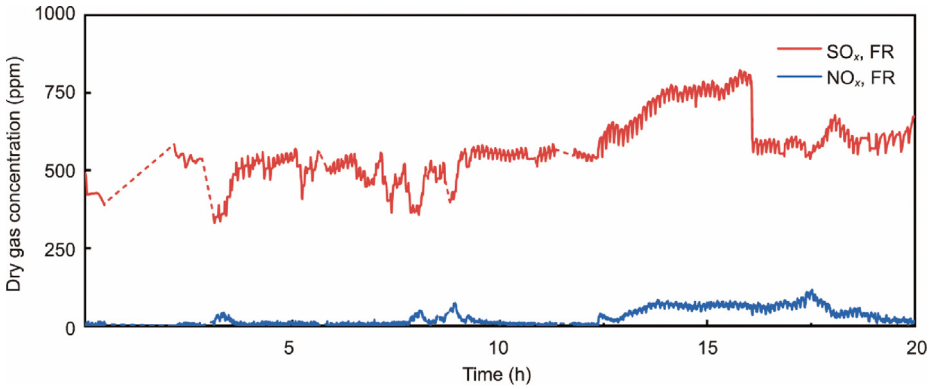


**Fig. 8.** $SO_2$ and $NO_x$ concentrations in the auto-thermal CLC mode.

in the AR. Therefore, we did not measure the concentrations of $SO_2$ and $NO_x$ from the AR outlet. The variation in the concentrations of $SO_2$ and $NO_x$ from the FR outlet is shown in Fig. 8, where it can be seen that the $SO_2$ concentration is in the range of 332–815 parts per million (ppm; dry basis), and the $NO_x$ concentration is in the range of 0–101 ppm (dry basis).

In a reducing atmosphere, the sulfur in coal can be released as $H_2S$, COS, and $SO_2$, while the nitrogen in coal can be released as $NH_3$ or HCN. The gas species of $H_2S$, COS, $NH_3$, and HCN can be oxidized by the OC to $SO_2$ and $NO_x$; therefore, the concentration of $SO_2$ and $NO_x$ is related to the oxidation valence of the OC. An OC with a high oxidation conversion will result in a high concentration of $NO_x$ in the FR, while an OC in a reduced state will result in a very low concentration of $NO_x$ in the FR. Therefore, the operational parameters significantly affect the $SO_2$ and $NO_x$ emissions from the FR; thus, it will be necessary to reduce the $SO_2$ and $NO_x$ emissions by optimizing the operational parameters in future studies.

## 4. Conclusions

A 5-$MW_{th}$ CLC pilot unit was successfully demonstrated in China with funding from China's MOST and the EU's Horizon 2020. The results of 20 h of auto-thermal CLC operation with lignite fuel were presented in this work, representing the real auto-thermal CLC tests: all the solid fuel was fed into the FR, and only air was fed into the AR, without any external heating. As a result, the whole pilot unit was heated by the heat released from the oxidation of the OC inside the AR. Lignite and ilmenite were respectively used as the solid fuel and the OC. The thermal input of the lignite was 3.5–5.0 $MW_{th}$, and the temperatures of the AR and the FR were 1000–1040 and 940–980 °C, respectively. The $CO_2$ concentration at the FR outlet was mainly in the range of 88%–96%, while the $CO_2$ concentration at the AR outlet was mainly below 2%. Based on the operational data, the maximum $CO_2$ capture efficiency of lignite was greater than 97%, and the minimum oxygen demand for unburnt gases from the FR was 2.45%. The AR had lower emissions of $SO_2$ and $NO_x$ because of a very small amount of char slipping into the AR; the $SO_2$ concentration was in the range of 332–815 ppm (dry basis) from the FR, and the $NO_x$ concentration was in the range of 0–101 ppm (dry basis) from the FR. It was found that the ratio of primary air in the AR and the bed inventory in the FR significantly affected the oxygen demand. To the best of our knowledge, this represents the first instance worldwide of achieving long-term auto-thermal operation of CLC with a high carbon capture efficiency (> 91%) and low oxygen demand (< 8%) on the megawatt scale. As such, this demonstration is a breakthrough in CLC technology toward achieving subsequent deployment in an industrial-integrated CCUS chain.

## CRediT authorship contribution statement

**Zhenshan Li:** Writing – review & editing, Project administration, Methodology, Funding acquisition, Conceptualization. **Yang Wang:** Writing – original draft, Methodology, Investigation, Data curation. **Weicheng Li:** Supervision, Resources. **Geng Wei:** Investigation. **Xinglei Liu:** Investigation. **Shanhu Lin:** Investigation. **Jiaye Li:** Investigation. **Dan Li:** Investigation. **Qingsong Meng:** Investigation. **Li Nie:** Supervision. **Vincent Gouraud:** Investigation. **Shuting Wei:** Investigation. **Patrice Font:** Investigation. **Nils Erland L. Haugen:** Project administration. **Øyvind Langørgen:**

Investigation. **Yngve Larring:** Investigation. **Zuoan Li:** Investigation. **Ningsheng Cai:** Supervision.

## Declaration of competing interest

The authors declare that they have no known competing financial interests or personal relationships that could have appeared to influence the work reported in this paper.

## Acknowledgment

This research was funded by National Key Research and Development Program of China (2024YFB4105904).

## Appendix A. Supplementary data

Supplementary data to this article can be found online at https://doi.org/10.1016/j.eng.2025.07.017.

## References

[1] State of the global climate 2023. Report. Geneva: World Meteorological Organization; 2024.
[2] The Paris agreement [Internet]. Bonn: United Nations Climate Change; [cited 2024 Dec 24]. Available from: https://unfccc.int/process-and-meetings/the-paris-agreement?gad_source=1&gclid=Cj0KCQiA1Km7BhC9ARIsAFZfEItU0Xcm86p36_aENCq9rPk1rMlAzMl1FHizEBWcVP42Iii8fDiVVYoaAkgnEALw_wcB.
[3] 2024 statistical review of world energy. Report. London: Energy Institute; 2024.
[4] World energy outlook 2024. Report. Paris: International Energy Agency; 2024.
[5] Chen S, Liu J, Zhang Q, Teng F, McLellan BC. A critical review on deployment planning and risk analysis of carbon capture, utilization, and storage (CCUS) toward carbon neutrality. Renew Sus Energy Rev 2022;167:112537.
[6] Dubey A, Arora A. Advancements in carbon capture technologies: a review. J Clean Prod 2022;373:133932.
[7] Carbon dioxide capture and storage. Report. Geneva: Intergovernmental Panel on Climate Change; 2005.
[8] Lyngfelt A, Leckner B. A 1000 $MW_{th}$ boiler for chemical-looping combustion of solid fuels—discussion of design and costs. Appl Energy 2015;157:475–87.
[9] Adánez J, Abad A, Mendiara T, Gayán P, De Diego LF, García-Labiano F. Chemical looping combustion of solid fuels. Prog Energy Combust Sci 2018;65:6–66.
[10] Richter HJ, Knoche KF. Reversibility of combustion processes. In: Efficiency and costing. Washington, DC: American Chemical Society; 1983. p. 71–85.
[11] Coppola A, Scala F. Chemical Looping for combustion of solid biomass: a review. Energy Fuel 2021;35:19248–65.
[12] Abdulally I, Beal C, Andrus H, Epple B, Lyngfelt A, Lani B. Alstom's chemical looping prototypes, program update. In: Proceedings of 37th International Technical Conference on Clean Coal & Fuel Systems; 2012 Jun 3–7; Clearwater, FL, USA. Gaithersburg: Coal Technologies Associates; 2012.
[13] Abdulally I, Beal C, Andrus H, Epple B, Lyngfelt A, White B. Alstom's chemical looping technology, program update. In: Proceedings of 11th Annual Conference on Carbon Capture Utilization & Sequestration; 2014, Pittsburgh, PA, USA.
[14] Ströhle J, Orth M, Epple B. Design and operation of a 1 $MW_{th}$ chemical looping plant. Appl Energy 2014;113:1490–5.
[15] Ohlemüller P, Busch JP, Reitz M, Ströhle J, Epple B. Chemical-looping combustion of hard coal: autothermal operation of a 1 $MW_{th}$ pilot plant. ASME J Energy Resour Tech 2016;138(4):042203.
[16] Baek JI, Choun M, Kim U, Lee G, Kim D, Ryu HJ. The K-CLC project: development of 3 $MW_{th}$ CLC steam generation system towards a clean power plant. In: Proceedings of the 16th International Conference on Greenhouse Gas Control Technologies (GHGT-16); 2022 Oct 23–27; Lyon, France. Cheltenham: IEAGHG; 2024.
[17] Zhao H, Tian X, Ma J, Chen X, Su M, Zheng C, et al. Chemical looping combustion of coal in China: comprehensive progress, remaining challenges, and potential opportunities. Energy Fuel 2020;34(6):6696–734.
[18] CORDIS—EU research results. Chinese–European emission-reducing solutions. Report. Brussels: European Commission; 2024.
[19] Haugen NEL, Li Z, Gouraud V, Bertholin S, Li W, Larring Y, et al. Building the world's largest chemical looping combustion (CLC) unit. Int J Greenh Gas Control 2023;129:103975.
[20] Leckner B. Fluidization characteristics of circulating fluidized bed boilers. Chem Ing Tech 2023;95:32–9.
[21] Li W, Li Z, Chen H, Liu X, Cai N, Zhang A, et al. Controlling the solid circulation rate and residence time in whole loops of a 1.5 $MW_{th}$ chemical looping combustion cold model. Energy Fuel 2022;36(17):9513–28.
[22] Liu L, Li Z, Li Z, Larring Y, Cai N. Heterogeneous reaction kinetics of a perovskite oxygen carrier for chemical looping combustion coupled with oxygen uncoupling. Chem Eng J 2021;417:128054.
[23] Liu L, Li Z, Wang Y, Li Z, Larring Y, Cai N. Industry-scale production of a perovskite oxide as oxygen carrier material in chemical looping. Chem Eng J 2022;431:134006.
[24] Li Y, Li Z, Liu L, Cai N. Measuring the fast oxidation kinetics of a manganese oxygen carrier using microfluidized bed thermogravimetric analysis. Chem Eng J 2020;385:123970.
[25] Chen H, Li Z, Wang R. Design theory of a CLC air reactor with oxygen carrier recirculation and its application to a 3 $MW_{th}$ pilot. Energy Fuel 2021;35(2):1580–93.
[26] Chen H, Li Z, Liu X, Li W, Cai N, Bertholin S, et al. Solid circulation study in a 1.5 $MW_{th}$ cold flow model of chemical looping combustion. Ind Eng Chem Res 2021;60:2265–77.
[27] Li Y, Wang H, Li W, Li Z, Cai N. $CO_2$ gasification of a lignite char in microfluidized bed thermogravimetric analysis for chemical looping combustion and chemical looping with oxygen uncoupling. Energy Fuel 2019;33(1):449–59.
[28] Gouraud V, Wei S, Zhang A, Vin N, Font P, Mendez DM, et al. CHEERS demonstration unit operational results for the European configuration. In: Proceedings of 17th International Conference on Greenhouse Gas Control Technologies (GHGT-17); 2024 Oct 20–24; Calgary, AB, Canada. Cheltenham: IEAGHG; 2024.
[29] Adánez J, Cuadrat A, Abad A, Gayán P, de Diego LF, García-Labiano F. Ilmenite activation during consecutive redox cycles in chemical-looping combustion. Energy Fuel 2010;24(2):1402–13.